

Fabrication and structural tuning of novel composite hollow fiber membranes for pervaporation

Jia Ming Zhu,¹ Ge Li,¹ Lan Ying Jiang^{1,2}

¹School of Metallurgy and Environment, Central South University, Changsha 410083, China

²National Engineering Research Center for Control and Treatment of Heavy Metal Pollution, Changsha 410083, China

Correspondence to: L. Y. Jiang (E-mail: jianglanyingsme@csu.edu.cn)

ABSTRACT: A series of polysiloxaneimide (PSI)/polyetherimide (PEI) composite hollow fibers were fabricated by coextrusion and phase inversion. The hydrophobic PSI outer layer was set as the selective layer which was supported by the PEI inner layer. The PSI was synthesized by polycondensation of 3,3',4,4'-Biphenyltetracarboxylic Dianhydride (BPDA) with amino siloxane X-22-161A and a chain extender, 1,3-Bis (3-aminopropyl) – 1,1,3,3-tertramethyldisiloxane (BATS). It was found that the macroscopic uniformity of PSI layer was dependent on the dope formulation, coagulant composition and dope flow rate: (1) the higher similarity degree of the solvent(s) for different layers in terms of solubility parameters, (2) the utilization of surfactant as a component in the water coagulant, and (3) higher flow rates of the outer layer dopes, led to the formation of more uniform and smoother PSI outer layer. The maximum outer layer thickness was around 2 μm . The bulk of the PEI layers were porous with finger like macrovoids. The outer surface of the inner PEI layer for some batches of the hollow fibers was confirmed to be porous. The original dual-layer hollow fibers showed poor pervaporation performance. Post treatment was applied to cure the hollow fiber, delivering composite membranes with performance dominated by the coating material of PDMS. © 2016 Wiley Periodicals, Inc. *J. Appl. Polym. Sci.* **2016**, *133*, 43324.

KEYWORDS: composite membrane; pervaporation; polysiloxaneimide; structure adjustment; uniformity of selective layer

Received 10 August 2015; accepted 6 December 2015

DOI: 10.1002/app.43324

INTRODUCTION

Pervaporation (PV) is a membrane technology commercialized in 1980s^{1,2} and it has been viewed as one of the most promising technologies in molecular level liquid separation. Its advantages include high separation efficiency, compact operation space and low energy consumption. It is especially attractive to the separations of liquids forming azeotrope or having closing boiling points.³

Hydrophobic pervaporation preferentially removes volatile organic compounds (VOCs) and has potential applications in biofuels production and wastewater treatment.^{4,5} In recent years, the effort on hydrophobic pervaporation has been intensified, as indicated by the increased accumulation of publications in past few years. Membrane material and formation are among the factors essential to economical application and remains to be one of the research focuses. Polydimethylsiloxane (PDMS) is a widely used material for preparing hydrophobic pervaporation membranes.^{4–7} Several strategies such as block/graft copolymerization,^{8,9} polymer blending,¹⁰ and organic/inorganic mixed matrix materials,¹¹ are developed to create new membrane materials that combine the hydrophobicity of PDMS and the

special properties of other compounds. Polysiloxaneimide (PSI) is a copolymer composed of PDMS and polyimides (PI) segments. The mechanical strength of PSI is higher than, while its permeability is almost on the same order of magnitude as that of PDMS.¹² As demonstrated in many works,^{13,14} PSI materials also possess good pervaporation performance in organic/water separation. In Chang *et al.*'s work, PSI membranes for pervaporation were synthesized from BTDA, 4,4'-(hexafluoroisopropylidene) diphthalic anhydride (6FDA) and pyromellitic dianhydride (PMDA) with PDMS (SIDA $M_n = 800$ g/mol).¹³ In Krea *et al.*'s work,¹⁴ the average molecular weight of the PSI copolymers prepared from PDMS (ODMS $M_n = 900 - 5000$ g/mol) were significantly improved by incorporating 1,3-bis (3-aminopropyl) tetramethyldisiloxane (MDMS) as a chain extender. The highest separation factor for phenol recovery from its 5 wt % aqueous solution was 22 with a membrane containing 6FDA and 89 wt % PDMS. Jiang *et al.* prepared organophilic pervaporation film using PSI synthesized from 2,2'-bis[4-(4-aminophenoxy) phenyl] hexafluoropropane (BDAF), 4,4'-(hexafluoroisopropylidene) diphthalic anhydride (6FDA), and diamine-terminated poly(dimethyl siloxane)s.¹² The PSI with SIDA of 4600 g/mol had both higher flux of (27.6 g/m²h) and separation factor (3270) in

treating 500 ppm trichloroethylene (TCE) at 25°C. A few recent reports have documented the production of polymer–inorganic filler mixed matrix membranes.^{15,16} Liu *et al.* filled silicalite into the PSI.¹⁵ These membranes showed a total flux of 280 g/m²h and a separation factor of 52.2 in recovering chloroform from water by pervaporation.

To facilitate the application of hydrophobic pervaporation, anisotropic membranes with generic properties of higher flux is necessitated.¹⁷ Generally, the mechanical strength of elastomers is not strong, which may cause the collapse of the self-support anisotropic membranes under actual pervaporation conditions. Therefore, composite structure is the principle choice in preparing hydrophobic pervaporation membranes. PSI/PEI/nonwoven fabric composite membranes using PSI as a selective layer for hydrophobic pervaporation were developed by Song and Jiang for the first time.¹⁸ The nonwoven fabric layer covered by a crosslinked porous polyetherimide (PEI) layer was employed as a mechanical support, on which the PSI layer was formed by nonsolvent induced phase inversion. The highest separation factor for ethanol/water separation by pervaporation was around 2.5. The flux of the membrane was low due to that the PSI layer was more than 20 μm thick.

In this study, PSI/PEI composite hollow fibers are prepared. The reason for developing hollow fiber is that this type of configuration has the merit of high packing density.^{19,20} The method utilized for the composite structure formation involves co extrusion coupled with dry-wet phase separation. The motivation for adopting this approach is that PSI share the same solvent with many glassy polymers suitable for porous support. A multi-step casting procedure will destroy the desired structure of prefabricated support layer when forming the PSI layer in the last step. Preparing two layers simultaneously, the problem may be circumvented. In addition, the one-step co-precipitation approach has several advantages that have been elaborated by other researchers.²¹ Among these points the most attractive one is the potentially higher membrane fluxes. With the single-step production, a sufficiently porous support structure will not suffer the migration of selective layer polymer into the pores of support. This point is in contrast with the characteristics of traditional composite membrane. One of the disadvantages associated with the latter is the pore intrusion by coating of functional layer material.²² The consequence is extra transport resistance and reduction in hydrophobic selection. This work will demonstrate for the first time the formation of composite hydrophobic pervaporation membranes by co-extrusion. The effects of spinning conditions such as dope flow rate, dope formulation, coagulant composition on the PSI/PEI dual-layer membrane morphologies will be investigated. The mechanisms underneath the relationships observed will be proposed and discussed. The pervaporation performance of the membrane fabricated will also be examined preliminarily.

EXPERIMENTAL

Materials

Polyetherimide (PEI) for support layer was purchased from Saudi Basic Industry Corp. (SABIC) and was dried *in vacuo* at 80°C for 12 h before being used. 3,3',4,4'-Biphenyltetracarboxylic dianhy-

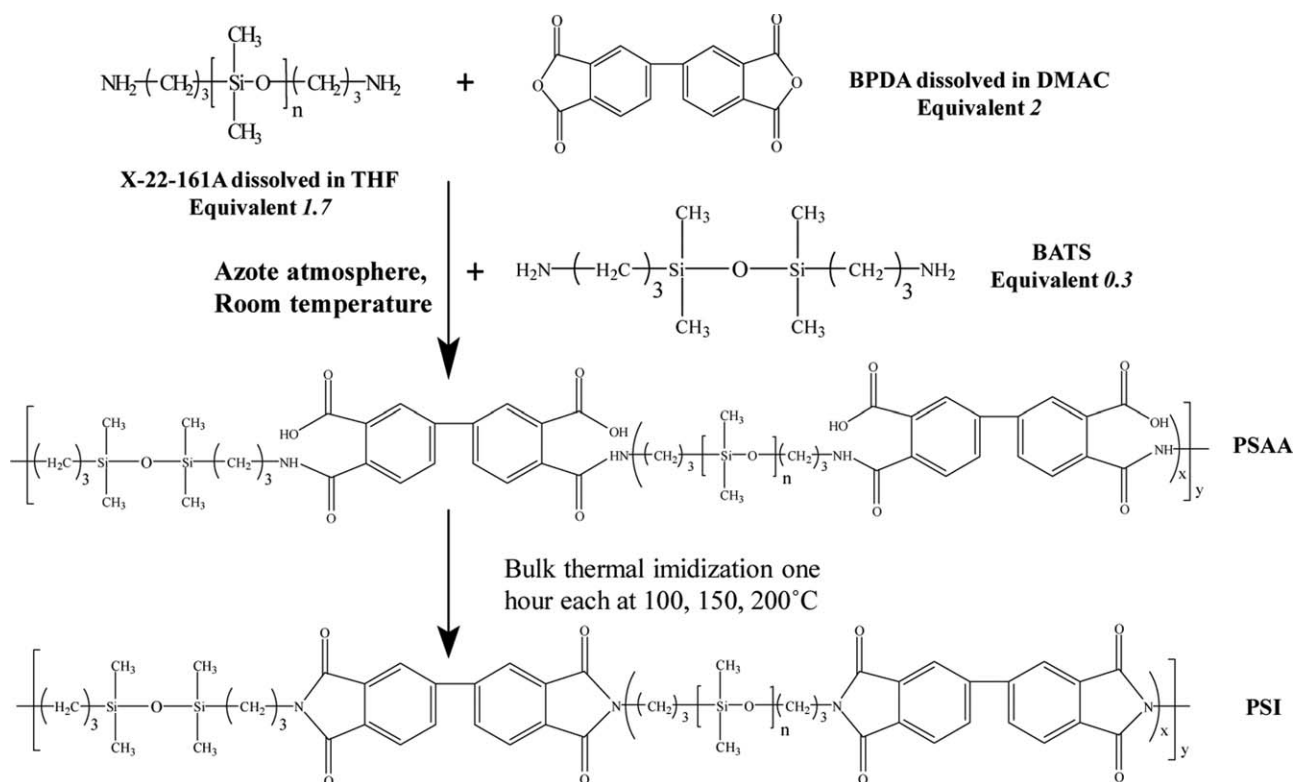
dride (BPDA) (97 wt %) was supplied by Sigma Aldrich Inc. Reactive polydimethylsiloxane (PDMS) with amino groups at both ends (amino group equivalent weight of 800g/mol) was from Shin-Etsu Chemical. Chain-extender 1,3-Bis (3-amino-propyl)–1,1,3,3-tertramethylidisiloxane (BATS) was purchased from Alfa Aesar Inc. Polyethylene glycol (PEG, Molecular weight (M_w) 800 g/mol) was provided by Tianjin Kemiou Chemical Reagent. High performance liquid chromatography (HPLC) grade tetrahydrofuran (THF) and *N*-dimethylacetamide (DMAc) for PSI synthesis were from Merck Specialities Ptd. Ltd. and *N*, Tianjin Kemiou Chemical Reagent, respectively. Analytical reagents (AR) grade THF from Changsha Huihong Chemical Reagent and *N*-methyl-2-pyrrolidone (NMP) from Sinopharm Chemical Regent for dope preparation were both of AR grade surfactant sodium dodecyl sulfate (SDS) was supplied by Sinopharm Chemical Regent. The chemical agents were used without further purification, unless otherwise specified. The PDMS kit of D184 was supplied by Dow Corning. The PDMS of WC107 was supplied by Wancheng Chemical, while the cross linker tetraethoxysilane (TEOS) and catalyst dibutyltin dilaurate (DBTDL) were purchased from Xilong Chemical and Aladdin Industrial Corporation, respectively. AR grade *n*-Hexane was from Sinopharm Chemical Reagent and used as received.

Polysiloxaneimide (PSI) Synthesis

The processes of PSI synthesis is illustrated in Scheme 1 in which the stoichiometric ratio of the monomers was shown as well. First, the BPDA was dissolved in DMAc with a concentration of 11.83 wt % purged by nitrogen (N₂). After 1 h, the PDMS solution in THF with a concentration of 73.50 wt % was slowly added into the BPDA solution through a constant pressure funnel. The resultant solution was magnetically stirred at 25°C with N₂ protection for 12 h. The BATS was then added into the mixture and the second reaction lasted for another 12 h under the same conditions as that in the first step. Polysiloxane amic acid (PSAA) was obtained after 24 h reaction. The concentration of PSAA in solvent mixture was 40 wt % and the weight ratio of the DMAc and THF was 4/1. Thereafter, the PSAA solution was poured into 1 L deionized water and left for 12 h. The precipitant of PSAA was taken out and dried *in vacuo* at 40°C for 12 h and then dissolved in THF. The procedure from precipitation to dissolution was repeated twice to remove the monomers and oligomers. The precursor PSAA was imidized under vacuum to form PSI. It was annealed at 100, 150, and 200°C for 1 h, respectively, and then cooled down naturally.

Preparation of PSI Films and PSI/PEI Hollow Fibers

The dense flat film of PSI was prepared using dry phase inversion method. First, 6 g PSI was dissolved in 54 g THF to obtain a 10 wt % PSI solution. The solution was poured into a Teflon disk with the diameter of 14 cm. The disk was covered by a glass plate for 1 day to allow the degassing of the solution. Afterward, a narrow gap was generated between the disk and the covering plate for solvent removal by vaporization. The naturally dried film was annealed for 10 hours at 100°C under vacuum. After being cooled down, the film was peeled off from the Teflon disk for follow-up tests.



The coextrusion and precipitation approach was employed for preparing the composite hollow fibers. The dope compositions and the flow rates for the inner layer, outer layer and bore fluid were tabulated in Table I. The PEI and PEG were dissolved in NMP at 80°C; the PSI or PSAA was dissolved in solvents at 40°C. The polymer/solvent mixtures were stirred continuously for 6 h to obtain homogenous dopes. Thereafter, the dopes were left in the tanks at 60°C for overnight degassing. The polymer solutions and the bore fluid were transferred from their storage tanks to the triple-orifice-spinneret. After coming out from the spinneret, the nascent fibers went through a specific

air gap and entered the external coagulant. The conditions of spinning were listed in Table II. Phase inversion was initiated by the external and internal coagulant and the newly formed fibers were taken up and collected by a roller. Subsequently, the fibers were soaked in tap water, which was replaced daily, for 3 days to remove the residual solvent. Thereafter, they were cut into shorter pieces of 30cm long and air dried.

Hollow Fiber Module and Post Treatment

The hollow fiber module was fabricated according the work by Song and Jiang.²³ Two stainless steel union tees were linked by

Table I. The Compositions and Flow Rates of Outer/Inner Layer Dopes and External/Internal Coagulants for the Dual-Layer Hollow Fiber Membranes

ID	Outer layer dope			Inner layer dope		Bore fluid		External coagulant
	Composition (wt %)	Flow rate (mL/min)		Composition (wt %)	Flow rate (mL/min)	Composition (wt %)	Flow rate (mL/min)	
S1	–	a	b	c	PEI/PEG800/NMP 15/5/80			Water
D1	PSI/THF 20/80							Water
D2	PSI/NMP/THF 20/40/40					2	Water/Ethanol 80/20	1.5 Water
D3	PSI/THF 20/80	0.02	0.05	0.1	PEI/PEG800/NMP 15/5/80			Sodium Dodecylsulfate/Water 0.2 w/v % (2 g/L)
D4	PSI/NMP/THF 20/40/40							Sodium Dodecylsulfate/Water 0.2 w/v % (2 g/L)

Table II. Dual-Layer Hollow Fiber Fabrication Conditions

Spinning conditions	Value
Humidity (%)	75
Spinneret temperature (°C)	Room Temperature
Bore fluid temperature (°C)	30
The inner layer dopes temperature (°C)	30
The outer layer dopes temperature (°C)	Room Temperature
External coagulant temperature (°C)	40
Take up speed	Free fall
Air gap (cm)	5

a plastic tube with a specific length and inner diameter of 4.0 mm. A piece of fiber was placed in the tube with both ends protruded from the union tee outlets. The space in the two ends between the fiber and the union tee was then sealed with fast epoxy and dried overnight. Epoxy was applied twice to ensure complete sealing. The effective length of the fiber was 16 cm.

The fiber for the pervaporation test was cured by the three kinds curing agents. For KFZ314 and D184, PDMS (A) and crosslinking agent (B) were blended with a ratio of 10/1. For treatment using WC107, it was mixed TEOS and DBTDL with a proportion of 10/1/0.2 by weight. Each curing agent was dissolved in n-hexane to form 3 wt % solution. The hollow fibers with two ends being were immersed into the PDMS solution for coating, and then taken out. After being dried in air naturally, the coated fibers were thermally treated at 60°C for 12 h in vacuum for deep drying and reinforcing crosslinking.

Characterizations

The morphology of the hollow fiber was examined by using the field emission scanning microscopy (FESEM) (FEI Electron Optics B.V. and Nova Nano SEM 230). To observe the cross section of the fibers, the samples were fractured in liquid N₂. The samples were dried in vacuum before SEM observation. Gold of nanoparticles was sprayed on the surface of samples for SEM to promote the electrical conductivity. The Energy Dispersive X-ray Spectroscopy (EDX) (JSM-6360LV/EDX-GENESIS) was employed to detect the elements distribution on the shell/lumen surfaces and cross section of the fibers. To characterize the outer/inner layers' interface morphology, the outer PSI layer was exfoliated by attaching the adhesive tape on the external surface, followed by peeling off the tape.

The sorption of pure water or ethanol in the PSI material was performed. The mass of the film samples dried under vacuum at 100°C for 2 h before the sorption test weighted and recorded. Then the film immersed in the liquid at 25°C and 60°C, respectively. The masses of the wetted samples were recorded in closed container after residual liquid on the sample surface was blotted by tissue paper. The swelling degree was calculated by the following equation:

$$S = \frac{m_2 - m_1}{m_1} \times 100\% \quad (1)$$

where, S is the swelling degree, m_1 and m_2 are the masses of dry sample and swollen sample.

Pervaporation and Sorption Test

Totally, 5 wt % ethanol/water mixtures were used for the PV test of neat PSI flat film and the device consulted the previous research.¹⁸ The stainless chamber, cold trap, and vacuum pump were successively connected by vacuum tube. The PSI dense film was set in a stainless membrane cell, and sealed by the rubber seal ring. On top side of the membrane, the feed solution kept at 45°C or 60°C controlled by a heat jacket and the solution was stirred by a magnetic stirrer. In the bottom chamber the membrane cell, a vacuum lower than 10 mbar was generated by a vacuum pump. The components transporting through the membrane was collected by cold trap immersed in liquid nitrogen. After 2 h of stabilization, the cold trap was exchange every 1~2 h for examining the sample collected. The mass of the sample was weighed by an electronic balance. The compositions were analyzed by gas chromatography system (GC-2011, Shandong Jinpu Analytical Instrument). Three duplicate analyses were applied for each sampling.

The total flux was calculated using the follow equation:

$$J_t = \frac{M}{At} \quad (2)$$

where, M (kg) is the total mass of liquid sample collected at permeate side, A is the effective membrane area in contact with the feed (m²), and t is the period time (h).

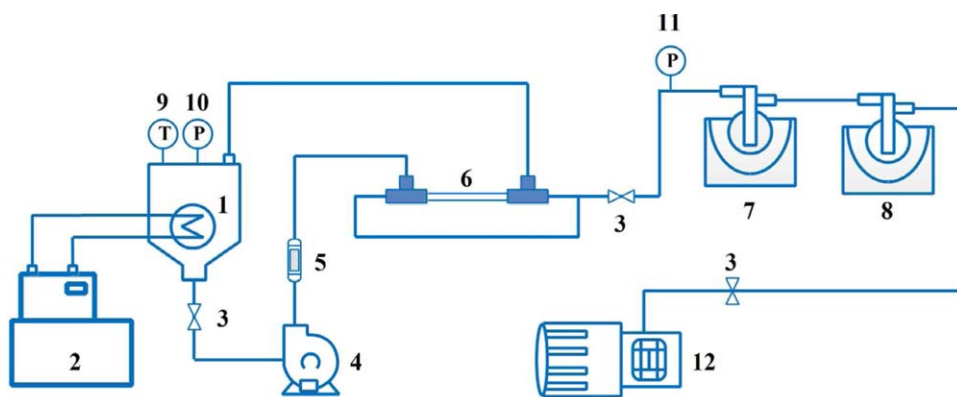
The separation factor of membrane was defined as:

$$\beta_{e/w} = \frac{y_e/y_w}{x_e/x_w} \times 100\% \quad (3)$$

where, x and y are the mole or mass fractions water (w) or ethanol (e) in feed and permeate, respectively.

Averages in flux and separation factor of all the samplings over a pervaporation duration of at least 4 hours were used as indicators for separation properties of the fiber. For every batch of hollow fiber, at least two parallel modules were prepared and tested.

The pervaporation test was also carried out for the hollow fiber membrane and the set up was shown in Scheme 2. The feed of 5/95 (w/w) ethanol/water mixture solution was stored in the feed tank and the temperature of the feed was monitored by the thermometer. The feed was heated by the thermostatic water tank and the temperature selected for pervaporation was 45°C or 60°C. Centrifugal pump was used to circulate the feed, of which the flow rate of was controlled at 100 L/h by the flow meter. The method for collection and characterization of the permeate was generally the same as that for PSI film. The only difference in the two operations is that the permeate sample for hollow fiber module was collected every 0.5~1 h after 0.5 h stabilization due to the much higher flux.



1. feed tank; 2. heating tank; 3. valve; 4. centrifugal pump; 5. flow meter;
6. membrane module; 7. cold trap I; 8. cold trap II; 9. thermometer;
10. pressure meter; 11. vacuum meter; 12. vacuum pump.

Scheme 2. The set up for the pervaporation test with hollow fiber. [Color figure can be viewed in the online issue, which is available at wileyonlinelibrary.com.]

RESULTS AND DISCUSSION

Characterizations of PSI Material

FTIR characterization confirms the imidization and the success of PSI synthesis. The PSI flat dense films experience the pervaporation tests for treating 5 wt % ethanol/water mixture solution at 45°C and 60°C, respectively. The graphs in Figure 1(A) show their pervaporation performance in terms of total flux

and separation factors under different feed temperature. As revealed, with the temperature being changed from 45 to 60°C, the pervaporation flux increases from 0.35 kg/m²-h to 0.44 kg/m²-h; meanwhile the separation factor increases from 1.36 to 1.74. Feed temperature not only influences the polymer chain mobility and free volume, but also the vapor pressure of organic and water, which bring about the performance variation

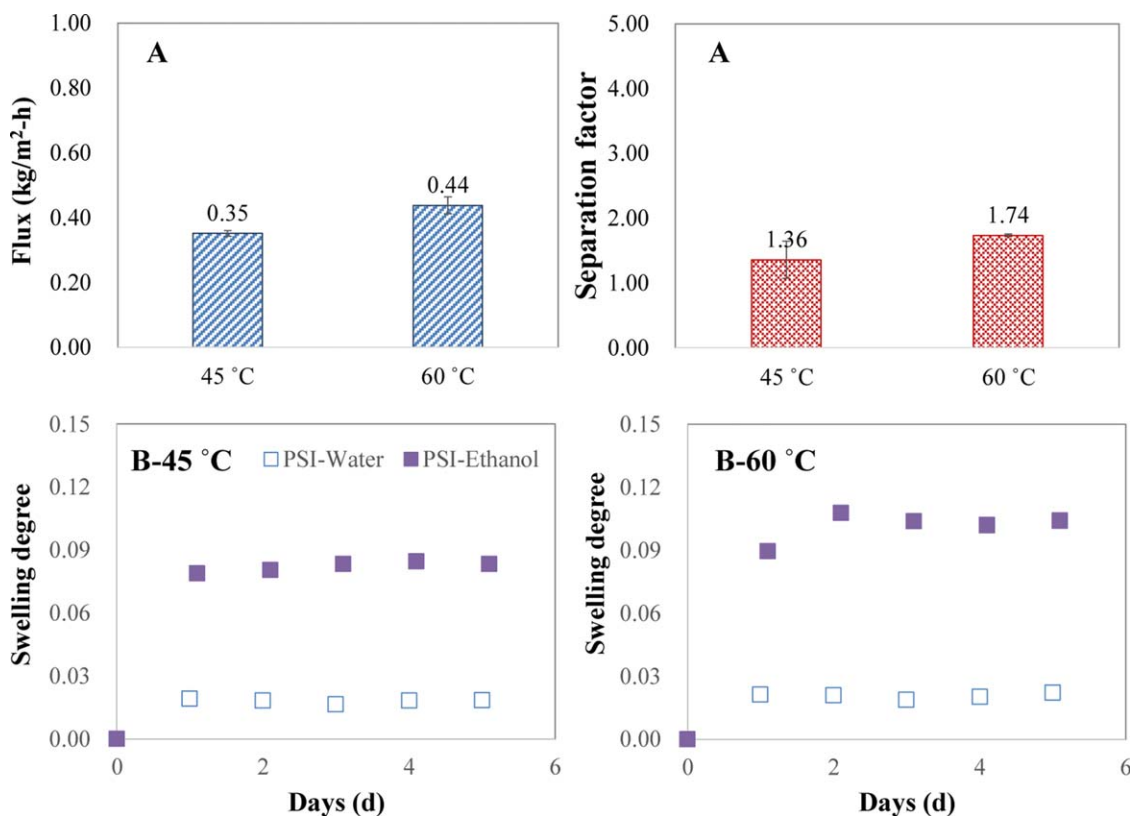


Figure 1. The pervaporation (A) and sorption (B) test of PSI flat dense film (thickness $\approx 280 \mu\text{m}$) at different feed temperatures. [Color figure can be viewed in the online issue, which is available at wileyonlinelibrary.com.]

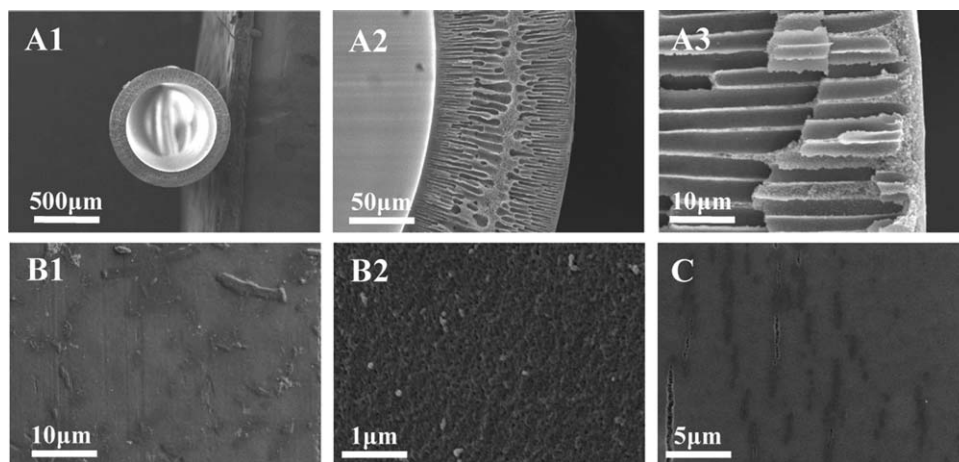


Figure 2. SEM pictures of the cross-section and the outer surface of the single-layer PEI hollow fiber S1. (A: cross-section; B: outer surface; C: inner surface).

observed. Similar trend was reported in several other researches.¹⁸ As shown in Figure 1(B), increasing the feed temperature promotes more the sorption of ethanol in the PSI material than that of water,¹⁸ which is a factor rendering the enhancement of the separation properties at higher temperature.

Morphology of Single-Layer PEI Hollow Fibers

The SEM pictures showing the morphologies of the single layer PEI hollow fiber (S1) are illustrated in Figure 2. The cross section exhibits two layer of densely distributed finger-like macrovoids initiating from inner and outer surfaces, respectively. Due to the hydrophilicity of PEI and the low concentration of the dope, instantaneous demixing favoring macrovoids' growth dominates the phase inversion.²⁴ In addition, PEG addition enhances the thermodynamical instability of the solution and water is a strong coagulant, which further strengthen the trend. The shapes of both layers of macrovoids are thin and sharp, and those distributed in the inner annulus are slightly longer. The phase inversion of the lumen side of the dope is introduced immediately after dope extrusion from spinneret orifice, while the demixing due to external coagulant happens after the nas-

cent fiber transports through the air gap. This situation allows the phase separation initiating from the lumen surface to develop more fully, leading to macrovoids with bigger size. Another reason may be the radial shrinkage of the fibers facilitates the coagulant intrusion from lumen side whereby the macrovoids becomes bigger.^{25,26} Figure 2 also displays the outer surface of the hollow fiber S1. Pores with diameters less than $0.05\mu\text{m}$ are observed on the shell surface and the inner surface is fully porous.

Tuning of PSI Layer Integrity for the Dual-Layer Hollow Fibers

Effects of PSI Outer Layer Dope Flow Rate. The SEM pictures in Figure 3 show the cross-section morphology of the D1 series hollow fibers. The PEI inner layers for these fibers are prepared using the same dopant and spinning conditions that are identical to the PEI single layer hollow fiber. Observation reveals that the cross-section of fiber D1b is obviously different from those of D1a. Unlike the latter, it has a distinct dense layer near the outer surface. Elemental analysis by EDX linescanning indicates that this layer contains silicon (S_i), and thus is composed of PSI. No S_i signal is identified near the outer surface of D1a at

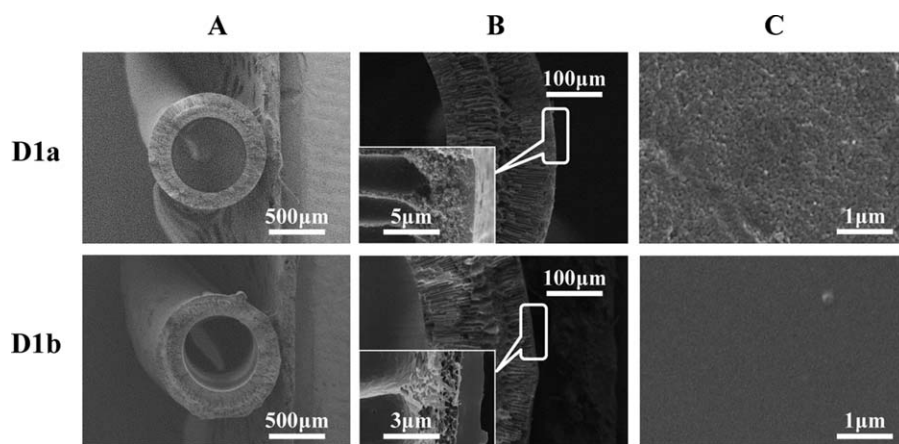


Figure 3. SEM pictures for the cross-section and outer surface of D1 series hollow fiber (A: overall cross-section; B: one eighth cross-section; C: outer surface).

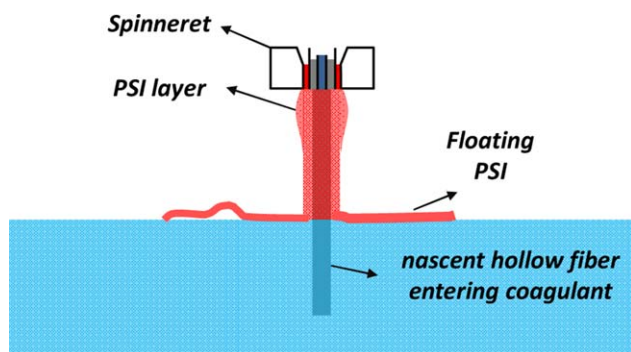


Figure 4. The pictures showing the situations near the spinneret exit for the nascent fibers of D1b, D2c, and D3c. [Color figure can be viewed in the online issue, which is available at wileyonlinelibrary.com.]

the position selected for EDX analysis, which may be a proof confirming the non-existence of PSI layer.

The surface tension of water coagulant (72.8 mN/m) is greater than those of the PSI and THF (37.8 and 26.4 mN/m) forming the outer layer dope solution. Such a difference is big enough to overcome the interfacial tension between the two liquids. In addition, the solubility parameters of the two dopes exhibit an obvious level of dissimilarity, implying a relatively weak adhesion or low compatibility. When the flow rate of the outer layer is low or the thickness is thin, the outer dope is almost completely sheared off from the inner dope upon immersion into water coagulant, and spontaneously spread on the water surface. This phenomenon is schematically shown in Figure 4. Mohammadi *et al.*²⁷ reported a similar phenomenon which was utilized for preparing ultrathin dense Poly (ether-block-amide) film for

PV separation. As for a thicker outer layer with fiber D1b, the effect of surface tension may not overtake the effect of combined gravity and adhesive force exerted on the outer layer to completely remove the PSI layer. Consequently, a ultrathin and homogenous PSI layer comes into being.

Observation of pictures in Figure 3 also reveals that the shell surface of D1a is seemingly hard and rigid, characteristics of a glassy polymer membrane. The porous morphology in terms of pore size and distribution is quite similar to that of hollow fiber S1, with micro pores having diameters less than 0.1 μm . Whereas, the outer surface of D1b is soft and dense, typical of rubbery polymer. Another difference between the D1a and D1b hollow fibers is associated with the morphologies of the porous PEI layer. The feature of PEI cross-section for D1a is quite similar to that of single layer PEI hollow fiber S1. Without PSI layer, the D1a hollow fiber is actually reduced to a single-layer PEI hollow fiber. Under the same fabrication conditions, it will evolve into a membrane basically identical to S1. The mechanism for the formation of dense PSI layer has been introduced in our previous work.¹⁸

In contrast to D1a or S1, the macrovoids in the shell annulus of PEI layer for D1b are obviously shorter and wider than those existing in the lumen annulus. This is probably due to the delayed phase separation caused by the presence of a hydrophobic PSI layer between the PEI layer and water coagulant. The time sequence for the macroscopic evolution of the PEI and PSI dopes after immersion into water coagulant is demonstrated in Figure 5. Instantaneous demixing favoring macrovoids formation happens with PEI solution, as indicated by its immediate transition from transparency to opaqueness. For PSI solution,

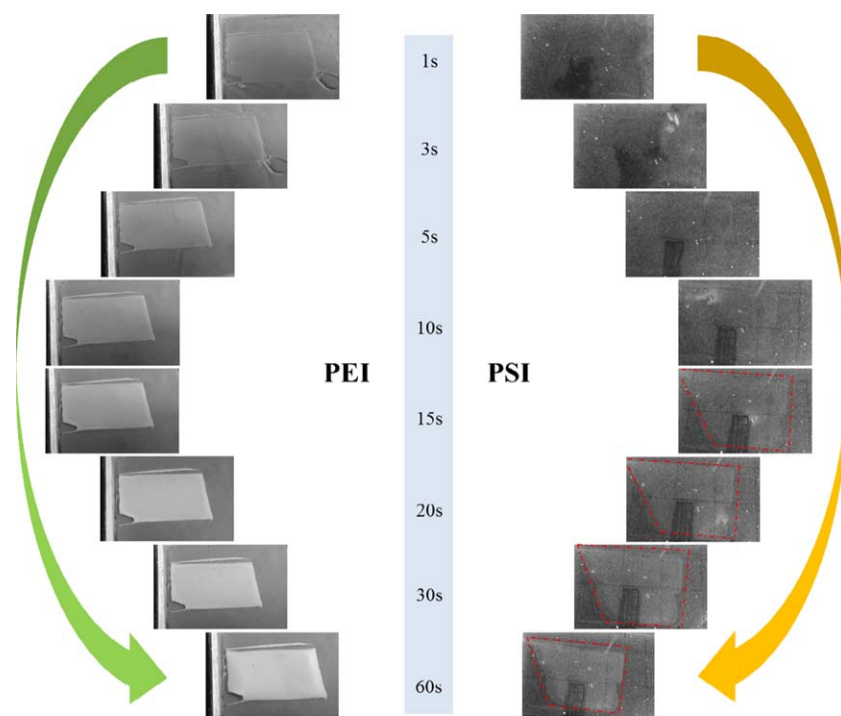


Figure 5. The time sequence of the evolution of the PEI and PSI dopes in film form after immersion into water. [Color figure can be viewed in the online issue, which is available at wileyonlinelibrary.com.]

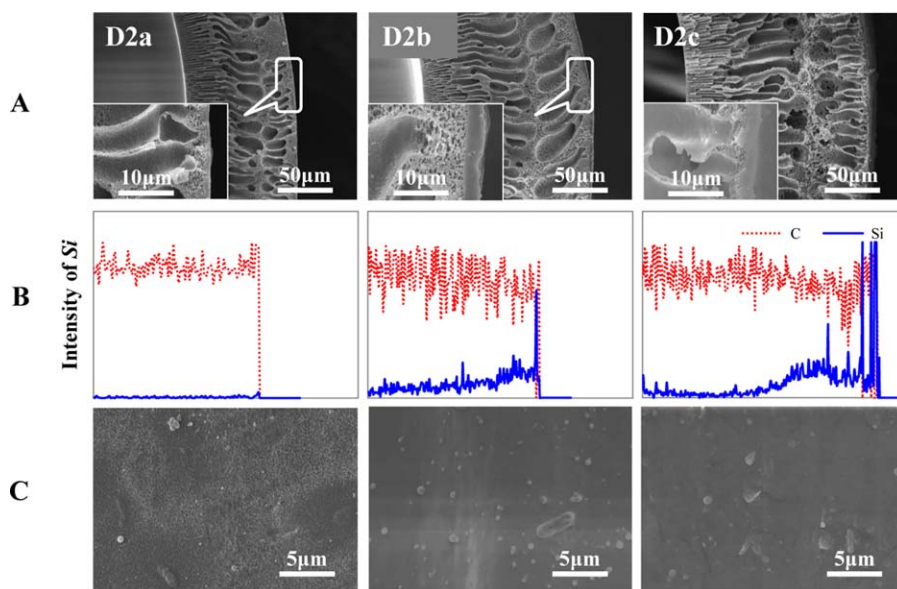


Figure 6. The SEM pictures and EDX analysis showing the morphologies of D2 series hollow fibers (A: cross-section SEM; B: EDX analysis; C: shell surface SEM). [Color figure can be viewed in the online issue, which is available at wileyonlinelibrary.com.]

the obvious change of its pellucidity is delayed to around 15s after contacting coagulant. Due to the higher hydrophobicity of PSI, water solution and diffusion through its matrix is slow, which also retards the phase inversion rate of the substrate PEI in the dual-layer hollow fiber. That is one of the reasons for the macrovoids shape deviation for hollow fiber containing an evident PSI layer.

Effect of Solvent Type for PSI Layer. Based on the discussion related to the PSI outer layer control in the above section, the ways to solve the problem are proposed. The first method is to promote the adhesive force by generating stronger compatibility between the PSI and the PEI dopes. Since NMP is the solvent for the inner layer, using mixed solvents containing NMP for outer layer PSI solution is considered to reduce the difference of solubility parameters between the inner and outer layer dopes. It was expected that higher compatibility between the two dopes by using common solvent might facilitate the formation of a PSI layer with continuity and homogeneity.²⁸ PSI can dissolve in THF well, whereas is insoluble in NMP. For the binary solvents selected, only an NMP/THF ratio of 1:1 leads to dissolution of PSI. The solubility parameters were calculated by the group contribution method²⁹ using the structural formula in Scheme 1 and inquired from the references.^{30–32} The solubility parameters of NMP, THF, and PSI are 23.10, 18.60, and 17.48 MPa^{1/2}, respectively. The smaller difference in solubility parameters between PSI and THF give rise to better dissolution of PSI in mixed solvent with relatively higher THF content.²⁸ Finally, THF/NMP with a ratio of 1:1 by weight is employed for preparing the dope of PSI layer.

Figure 6 summarizes the SEM pictures showing the morphologies of the D2 series of PSI/PEI dual-layer composite hollow fibers. The solvent for PSI layer in D2 series is THF and NMP mixture with ratio of 1:1 by weight. The comparison of Figures

3 and 6 informs us of the effect of PSI layer solvent type on its morphology. When the outer layer dope flow rate is fixed at 0.02 mL/min, the PSI layer cannot be observed in the SEM pictures with lower magnification. In the picture with higher magnification shown in the lower left corner, an irregular and scrap structure is identified near the external side of the fiber and seemingly not an integral part of the PEI layer. The above findings are corroborated by the EDX analysis locating beneath the SEM pictures for crosssection. Obvious and strong Si signal appears near the external surface of D2b and D2c fibers, and for D2a fiber only a trivial signal. Further observation shows that the outer surfaces of D2a, b, and c are all dense. All the fibers show the cross section characterized of two layer of macrovoids with those near the shell side being shorter and wider than those in the lumen annulus. As aforementioned, this feature indicates delayed demixing in the outer annulus due to the existence of a hydrophobic PSI solution. This observation indirectly confirms that all the three batches of D2 fibers have a PSI layer developed on its outer surface.

The above findings suggest that the rule for surface morphology evolution in Figure 6 with PSI layer dope flow rate is almost the same as that in Figure 3. In other words, only higher outer layer dope flow rate leads to the formation of a distinct double-layer composite structure. Nonetheless, the mixed solvent makes some difference from pure THF by retaining partially an ultrathin PSI layer on the shell side of fibers with lowest PSI dope flow rate. In addition to the solubilities being drawn closer for the two layers to promote adhesion of the two layers at interface, the following factors may also facilitate the evolution of a thin PSI layer with the lowest dope flow rate. The surface tension of the PSI solution using NMP/THF mixed solvent is 40.7 mN/m, more closer to that of water³³ than that using pure THF (i.e., 26.4 mN/m). At the same time, the viscosities of NMP and THF at 20°C are 1.7cp and 0.48cp, respectively.³³ The

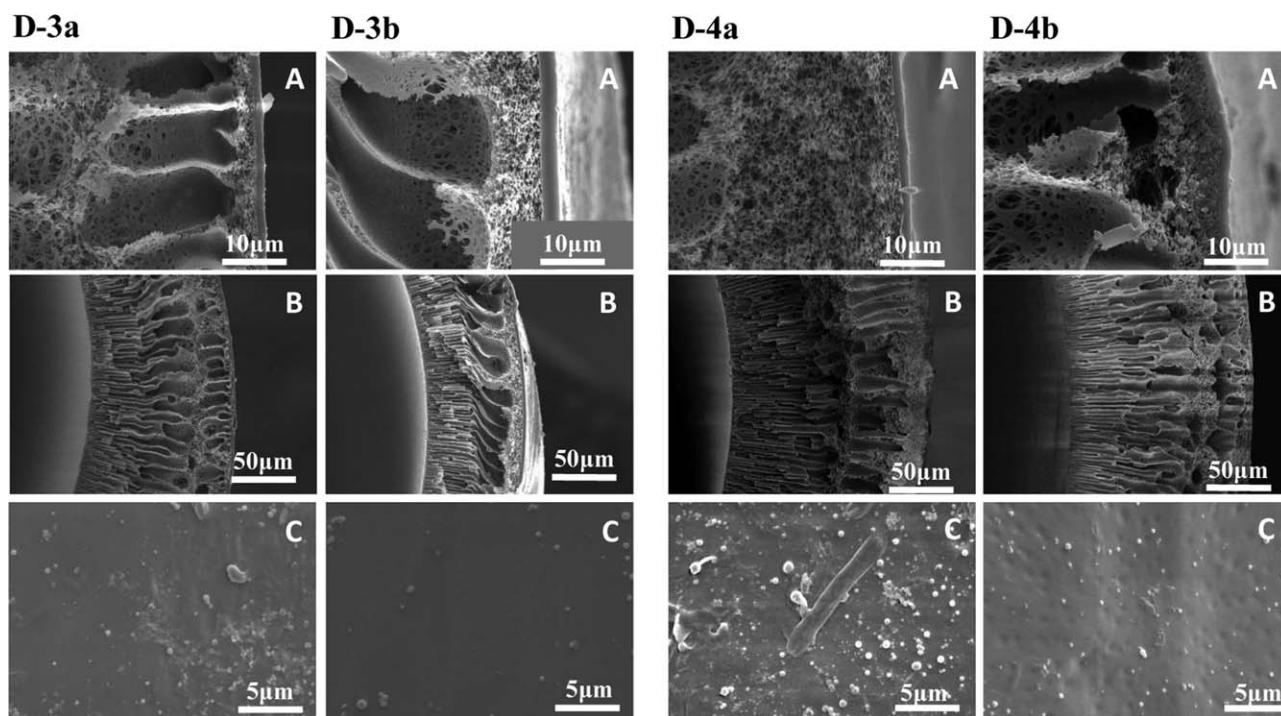


Figure 7. The cross-section and shell surface SEM pictures of D3 and D4 series hollow fibers with different magnifications (A: cross-section beneath outer layer; B: one eighth cross-section; C: outer surface).

usage of NMP in PSI dope will induce higher viscosity; hence, higher shear strength that is more resistant to surface tension effect.

Effect of Coagulant Composition. The findings in the above two sections show that the integrity of PSI layer cannot be achieved easily when attempting to further decreasing its thickness. Therefore, effort is directed towards the modification of coagulant surface tension by adding surfactant.³⁴ Based on the data of surface tension it is also found that a concentration of 2 g/L Sodium Dodecyl Sulfate water solution exhibit a surface tension of 47.69 mN/m, much lower than 72.84 mN/m of pure water. More importantly, the former value is significantly closer to the surface tensions of PSI dopes with both single THF and mixed solvent, which are 34.4 mN/m and 29.68 mN/m, respectively. In light of this comparison, the addition of surfactant is anticipated to hinder the delamination the PSI layer more easily and efficiently.

The morphologies of D3 and D4 series hollow fibers using coagulant containing surfactant Sodium Dodecyl Sulfate are demonstrated in Figure 7. For both series of hollow fibers, an ultrathin and almost uniform dense layer of around 1 μm verified to be PSI by elemental analysis is observed even when the PSI dope flow rate is reduced to 0.02 mL/min. The outer surfaces of these fibers are all dense. In addition, the cross-sections of all these fibers are featured with significantly shorter macrovoids in the outer annulus, implying the phase inversion dominated by delayed demixing mechanism near the outer surface. This is caused by the presence of a PSI layer at the outer surface, as aforementioned. Based on Figure 7, it is also found that

the boundaries of the two layers are distinctive and there exists no penetration of PSI into PEI layer.

Interface Morphology of the PSI/PEI Dual-Layer Hollow Fibers

For composite membrane it is desired that the support present minimum resistance to the mass transfer, which would require the support to be highly porous. Our previous work found that for the composite hollow fiber formed by co-extrusion, the outer surface of the inner layer developed quite compact structure which dominated the overall membrane separation efficiency.³⁵ The apparent cause for the evolution of such a structure was the solvent/nonsolvent concentration difference between the two layers. In this work, therefore, identical solvent concentration is applied for both dopes.

It was attempted to exfoliate the PSI layer from the PEI layer for observing the interface structure. Although the materials and dopes for each layer are different in surface tension and solubility parameter, the resultant hollow fiber exhibit no signs of delamination. The two layer attach to each other closely in the solidified hollow fiber, which makes it difficult to obtain sharply separated two layers. The strong attachment is due to two factors: (1) the PDMS segment is soft and can easily adapt to the topology of the support layer outer surface and immobilize on it; (2) there exists some dope solution interchange at the interface during membrane fabrication, leading to interpenetrating network to hook the two layers.

The morphologies of the structures exposed by the adhesive tape treatment illustrated in Figure 8. Figure 8(D1b) is quite dissimilar from Figure 3(D1b) before being treated, by showing seemingly porous structure with an average pore size around

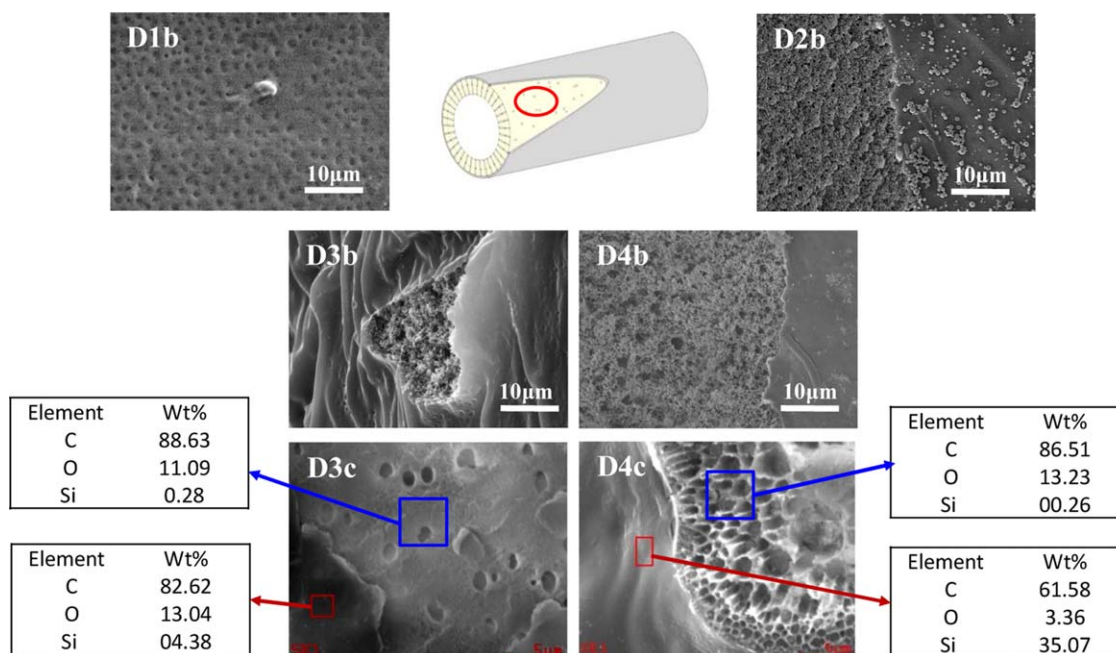


Figure 8. The interface morphologies of the hollow fibers by SEM and EDX analysis for different structures. [Color figure can be viewed in the online issue, which is available at wileyonlinelibrary.com.]

1 μm . Further observation of SEM of D1b in Figure 8 shows that these pores are not throughholes; in other words, there still a thin layer of PSI retained. As PSI layer of D1b is obviously dense, the porous structure is attributed to the PEI outer surface in contact with PSI. The PSI remains on the fiber after surface exfoliation is too soft to sustain itself. It collapses in the position where the pores locate, hence indirectly revealing the outline of the pores. Figure 9(D3c) shows the elemental analysis by EDX alongside the SEM observation for fiber D3c subject to surface treatment. Two distinctive morphologies are observed on its surface; namely, a porous section and a dense section. EDX analysis shows that the dense portion contains appreciable content of S_p , indicating the existence of PSI. Whereas, the content of S_i in the porous part is negligible, suggesting almost complete removal of the PSI from the PEI layer. The apparent

smoothness and lattice structure of D3c in the porous part are taken as denotation that the outer surface of the PEI inner layer is almost intact during the surface treatment.

Comparison of morphologies of D1b and D3c in Figure 9 shows that the pores of the two batches of fibers are of similar size, and both are much bigger than that of neat PEI hollow fibers S1 as shown in Figure 3 formed using the same PEI dope. The presence of the PSI layer slows down the penetration rate of coagulant, which in turn renders delayed phase separation favoring formation of larger pores on PEI side at the interface. Since the two dope solutions are quite different in their physicochemical properties, they take dissimilar phase inversion routes at the interface, resulting in a porous PEI surface while a dense PSI.

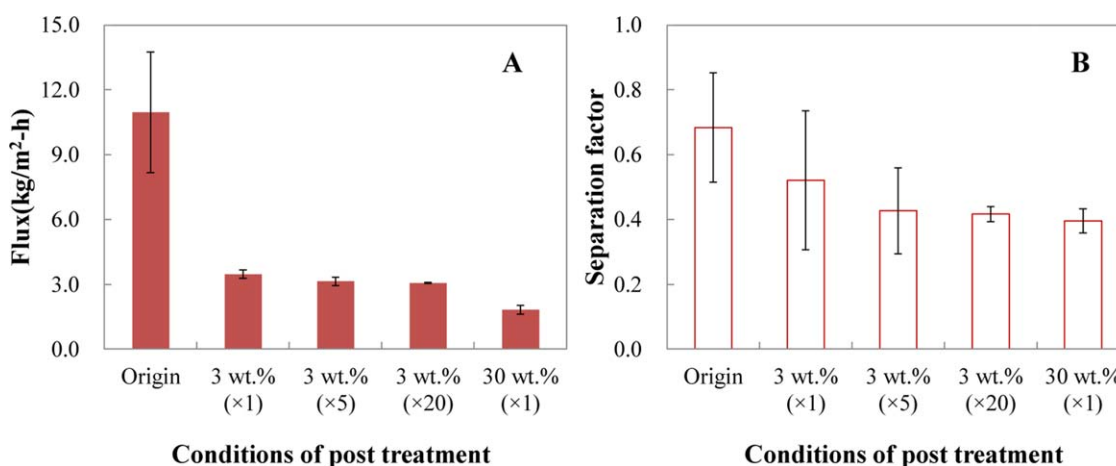
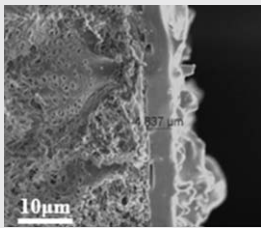
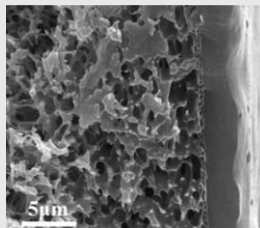
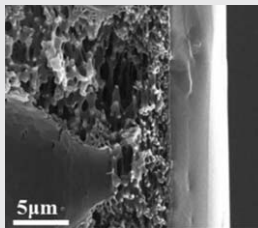
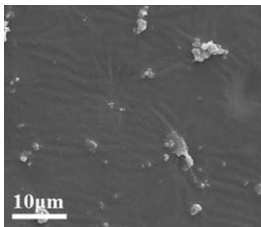
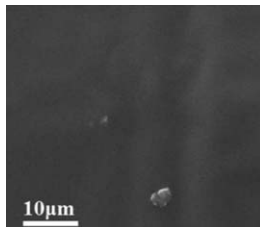
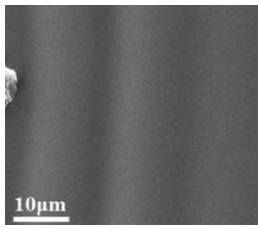


Figure 9. The flux (A) and the separation factor (B) for D4c fiber with different post treatment. (The number in the blanket means the number of coating for the post treatment). [Color figure can be viewed in the online issue, which is available at wileyonlinelibrary.com.]

Table III. The Cross Section and Surface Morphologies of the Hollow Fiber after Being Coated under Different Conditions

Coating conditions	PDMS conc: 3 wt %, coating number: 1	PDMS conc: 3 wt %, coating number: 20	PDMS conc: 30 wt %, coating number: 1
Cross section morphologies			
External surface morphologies			

In the other SEM pictures, quite porous but also rough structures are exposed after surface treatment. With EDX analysis it is found that no S_i is identified on the porous part, implying that it belongs to PEI support. However, it is not easy to discern whether they are the structures at the interface in direct contact with PSI layer, or of the interior part of PEI layer. Since PSI and PEI attach to each other intimately at the interface, the outer surface of PEI layer may be pulled away along with PSI layer during the surface treatment to reveal in effect the interior structure of PEI layer, instead of the interface structure.

Pervaporation Performance

Figure 9 shows the pervaporation performance of hollow fibers based on D4c at 20°C. As can be observed in Figure 9, the original or untreated D4c hollow fiber exhibits an average flux of around 11 kg/m²-h and a separation factor of 0.68 at 60°C. The thickness of PSI layer in the D4c fiber is ca. 2.0 μm of which if defect-free the flux is expected to be around 16 kg/m²-h based on the resistance model. This value is higher than that of the composite membrane. Though the PSI layer of fiber D4c looks dense, the separation factor indicates a separation process selective towards water with composite membrane, in contrast to that obtained with neat PSI film shown in Figure 1. Such a phenomenon as lower separation factor for anisotropic membrane than intrinsic value of membrane material is sometimes attributed to the existence of pin-hole in the skin layer.¹⁸ Considering the flux and the separation comparison mentioned above, the resistance of the hydrophilic PEI layer cannot be ignored. In effect, several work has reported that the support layer structure

can affect or even dominate the mass transport of a composite membrane for hydrophobic pervaporation.^{18,36}

Further work therefore is attempted to improve the membrane separation efficiency. Increasing the thickness of the PSI layer to make it dominate the transport of the dual-layer hollow fiber is one solution. The SEM pictures in Figures (3 and 6), and 7 signify that no obvious intrusion of PSI into the PEI layer occurs. Therefore, utilization of the PSI layer as an intermediate or gutter layer for a multi-layer composite membrane is considered.³⁷ Directly coating the selective material on porous support often results in a performance characterized of support material. The pore-free and highly permeable intermediate layer could prevent the occurrence of this situation.^{12–15} In this work, the multi-layer composite is fabricated by coating PDMS onto the PSI/PEI as support. According to the resistance model with increasing PDMS selective layer thickness, the selectivity will get closer to the values of the PDMS. The PDMS applied is D184 that has been investigated in several other researches about hydrophobic pervaporation.^{22,38} Figure 9 reveals the effect of the coating on the pervaporation performance of D4c hollow fiber. The conditions investigated include coating solution concentration and number of coating. The coatings under different conditions have all significantly reduced the flux 3–4 fold, from 11 kg/m²-h to less than 3 kg/m²-h. Observation of Figure 9 also tells that intensification of the coating by increasing coating number or concentration of the coating solution can further cause changes in the hollow fiber separation performance. The morphological characterization demonstrated in Table III indicates that the thickness of the PDMS coating increases obviously with the

Table IV. The Flux and the Separation Factor for D184 Flat Film

	Post thermal treatment	Thickness (μm)	60°C	
			Flux (kg/m ² -h)	Separation factor
D184	130°C for 1 h, 60°C for 12h at vacuum	≈287	0.49	0.28

coating intensity. This is one of the reasons for the flux depression. Since the thickness increment is not in proportion to the coating intensity, the depression in flux is not in linear relationship with the coating conditions. Regarding the separation factor, it also decreases after the fibers are coated. This observation is found to be associated with the intrinsic separation properties of the coating material.

The pervaporation performance of D184 PDMS material is shown in Table IV. The dense film of PDMS is prepared as follows: mixture of PDMS and crosslinking agent was cast on the surface of a glass plate by the scraper or casting knife. Then the nascent film was thermally treated under vacuum at 130°C for 1 h and 60°C for 12 h successively for crosslink. At last, the PDMS film was peeled off from the glass plate. Obviously shown in Table IV are that the PDMS material does not exhibit hydrophobic selectivity. Instead, it is slightly water selective. As a result, the coating superimposing extra resistance in a series manner is not capable to reverse the selectivity of the resultant multi-layer composite membrane. The EDX analysis in Figure 13 is about the coated hollow fiber. It is found that there is no obvious of S₂ element identified in the PEI layer, which confirm that the coating does not cause the penetration of the PDMS into the PEI support.

CONCLUSIONS

Hydrophobic PSI synthesized by polycondensation using three monomers (BPDA, BATS and amino-terminated PDMS) was used in fabrication of PSI/PEI dual-layer composite hollow fibers for the first time. The findings of the research are summarized below:

1. The PSI/PEI composite membranes were prepared by coextrusion and phase inversion. Several factors influenced the homogeneity and the integrity of the PSI layer: PSI dope flow rate, similarity of the solvents for the two dopes, and the composition of the external coagulant.
2. The PSI layer formed under different fabrication conditions was uniformly dense on the basis of the SEM characterization. Whereas, the outer surface of the PEI support was porous. The two layers had distinct boundary and no intrusion of PSI into the PEI happened.
3. The pervaporation performance of the PSI/PEI hollow fibers was slightly water selective. Probably the influence of the hydrophilic PEI layer cannot be ignored when the PSI layer is ultrathin.
4. PDMS coating was employed to form multi-layer composite hollow fibers. Due to that the intrinsic separation property of PDMS was water selectivity, the coated fibers were still favorable towards water transport. With higher intensity of coating, the separation factor approximated more the property of the PDMS material.

ACKNOWLEDGMENTS

The funding for the work includes National Natural Science Foundation of China (Project no. 21176265), Hunan Provincial Science and Technology Plan (Project no. 2014GK3106), and Chinese National Project for Overseas Experts in Culture, Education and Public Health (Account no. 140010001).

REFERENCES

1. Feng, X.; Huang, R. Y. M. *Ind. Eng. Chem. Res.* **1997**, *36*, 1048.
2. Rautenbach, R.; Albrecht, R. *J. Membr. Sci.* **1985**, *25*, 25.
3. Lipnizki, F.; Field, R. W.; Ten, P. J. *J. Membr. Sci.* **1999**, *153*, 183.
4. Vane, L. M. *J. Chem. Technol. Biotechnol.* **2005**, *80*, 603.
5. Huang, H. J.; Ramaswamy, S.; Tschirner, U. W.; Ramarao, B. V. *Sep. Purif. Technol.* **2008**, *62*, 1.
6. Jonquieres, Clement, A.; Lochon, R.; Neel, P.; Dresch, J.; Chretien, M. B. *J. Membr. Sci.* **2002**, *206*, 87.
7. Liu, D.; Liu, G.; Meng, L.; Dong, Z.; Huang, K.; Jin, W. *Sep. Purif. Technol.* **2015**, *146*, 24.
8. Wen, J.; Somorjai, G.; Lim, F.; Ward, R. *Macromolecules* **1997**, *30*, 7206.
9. Shinoda, H.; Miller, P. J.; Matyjaszewski, K. *Macromolecules* **2001**, *34*, 3186.
10. Hu, Y.; Wang, Y.; Gong, X.; Gong, X.; Zhang, X.; Jiang, W.; Zhang, P.; Chen, Z. *Int. J. Mod. Phys. B* **2005**, *19*, 1114.
11. Samanta, H. S.; Ray, S. K. *Purif. Technol.* **2015**, *146*, 176.
12. Jiang, X.; Gu, J.; Shen, Y.; Wang, S.; Tian, X. *Desalination* **2011**, *265*, 74.
13. Chang, Y. H.; Kim, J. H.; Lee, S. B.; Rhee, H. W. *J. Appl. Polym. Sci.* **2000**, *77*, 2691.
14. Krea, M.; Roizard, D.; Moulai-Mostefa, N.; Sacco, D. *J. Membr. Sci.* **2004**, *241*, 55.
15. Liu, Q. L.; Xiao, H. *J. Membr. Sci.* **2004**, *230*, 121.
16. Pechar, T. W.; Kim, S.; Vaughan, B.; Marand, E.; Baranauskas, V.; Riffle, J.; Jeong, H. K.; Tsapatsis, M. *J. Membr. Sci.* **2006**, *277*, 210.
17. Mao, Z.; Jie, X.; Cao, Y.; Wang, L.; Li, M.; Yuan, Q. *Sep. Purif. Technol.* **2011**, *77*, 179.
18. Song, Z. W.; Zhu, J. M.; Jiang, L. Y. *J. Membr. Sci.* **2014**, *472*, 77.
19. Matsuura, T. *Synthetic Membranes and Membrane Separation Processes*; CRC Press, **1993**.
20. Jiang, L. Y.; Chung, T. S.; Rajagopalan, R. *Chem. Eng. Sci.* **2008**, *63*, 204.
21. Jiang, L. Y.; Wang, Y.; Chung, T. S.; Qiao, X. Y.; Lai, J. Y. *Prog. Polym. Sci.* **2009**, *34*,
22. Vankelecom, I. F. J.; Moermans, B.; Verschuere, G.; Jacobs, P. A. *J. Membr. Sci.* **1999**, *158*, 289.
23. Song, Z. W.; Jiang, L. Y. *Chem. Eng. Sci.* **2013**, *101*, 130.
24. Peng, N.; Chung, T. S.; Wang, K. Y. *J. Membr. Sci.* **2008**, *318*, 363.
25. Jiang, L. Y.; Chung, T. S.; Cao, C.; Huang, Z.; Kulprathipanja, S. *J. Membr. Sci.* **2005**, *252*, 89.
26. Sukitpaneenit, P.; Tai-Shung, C. *J. Membr. Sci.* **2011**, *374*, 67.
27. Mohammadi, T.; Kikhavandi, T.; Moghbeli, M. *J. Appl. Polym. Sci.* **2008**, *107*, 1917.
28. Barton, A. F. *Chem. Rev.* **1975**, *75*, 731.

29. Park, K. A.; Lee, H. J.; Hong, I. K. *J. Ind. Eng. Chem.* **2010**, *16*, 490.
30. Chung, T. S.; Xu, Z. L. *J. Membr. Sci.* **1998**, *147*, 35.
31. Xu, J.; Xu, Z. L. *J. Membr. Sci.* **2002**, *208*, 203.
32. Pillin, I.; Montrelay, N.; Grohens, Y. *Polymer* **2006**, *47*, 4676.
33. E. W. Flick, *Industrial Solvents Handbook*; Noyes Publications, **1985**.
34. Qin, F.; Li, S. F.; Qin, P. Y.; Karim, M. N.; Tan, T. W. *Green Chem.* **2014**, *16*, 1262.
35. Jiang, L. Y.; Song, Z. W. *J. Polym. Res.* **2011**, *18*, 2505.
36. de Bruijn, F. T.; Sun, L.; Olujic, Z.; Jansens, P. J.; Kapteijn, F. *J. Membr. Sci.* **2003**, *223*, 141.
37. Peter, J.; Peinemann, K. V. *J. Membr. Sci.* **2009**, *340*, 62.
38. Zhang, Y.; Le, N. L.; Chung, T. S.; Wang, Y. *Chem. Eng. Sci.* **2014**, *118*, 173.